Acoustic Determination of Thermophysical Properties and Critical Parameters for R410A and Critical Line of xCO$_2$ + (1 − x)R410A

Nuno Ribeiro, Tânia Costa, Ana Aguiar-Ricardo, José M. S. S. Esperança, Pedro F. Pires,[†] and Henrique J. R. Guedes*

REQUIMTE/CQFB, Departamento de Química, Faculdade de Ciências e Tecnologia, Universidade Nova de Lisboa, Campus de Caparica, 2829-516 Caparica, Portugal

The thermophysical properties and critical parameters for the alternative refrigerant R410A (a near azeotropic refrigerant mixture containing difluoromethane (R32) and pentafluoroethane (R125) (50 wt % of each)) were investigated using two different acoustic techniques. The critical behavior of the system xCO$_2$ + (1 − x)R410A was also investigated. Experimental data of speed of sound in liquid R410A from (253 to 338) K and pressures up to 65 MPa were measured using a pulse-echo method. Derived thermodynamic properties were calculated, combining our experimental data with density and isobaric heat capacity values published by other authors. Measurements of the critical temperature T_c and pressure p_c on (R410A) and mixtures of xCO$_2$ + (1 − x)R410A were performed using another simple ultrasonic time-delay technique. The binary critical line was determined over the whole composition range, showing that this system deviates only slightly from ideality since the critical line is a continuous line. The Peng–Robinson equation of state with conventional mixing and combining rules was used to correlate the binary experimental data.

Introduction

Fluorinated alkanes (HFCs) represent the vast majority of chlorofluorocarbon (CFCs) and hydrochlorofluorocarbon (HCFC) substitutes. The technical challenges of the CFC phase-out are mostly overcome, but the HCFC phase-out cannot be regarded as finalized.

R410A, is a near azeotropic refrigerant mixture containing 50 wt % of pentafluoroethane (R125) + 50 wt % of difluoromethane (R32), that can be used as a substitute for R22 and also R13B1. One of the characteristics of the refrigerant R410A is its high vapor pressure, which, when applied to a heat pump, has led to significantly improved refrigerating capacity as compared to R22, R407C, and even propane. Results show that the use of R410A in optimized systems will increase the coefficient of performance when compared to R22, allowing the reduction of the overall costs when compared to other fluids. Also, the environmentally friendly R410A enjoys an important advantage because of the reduction in equipment size.[1] In other words, it is a high-pressure/high-efficiency refrigerant of the future, which in the long term is considered to replace R22.[2–4] The R32/125 system is perhaps the most widely studied system of all mixtures that have ever been measured, even compared to the well-measured systems methane/ethane, nitrogen/argon, and dry air. The data span the entire composition range and were measured at temperatures and pressures that cover nearly the entire range of practical fluid states.[5,6] As to environmental aspects, it has zero ozone depletion potential and a halocarbon global warming potential similar to R22. Despite being considered one of the most suitable HFC replacements for R22, there are few property measurements of the liquid phase reported, namely, the speed of sound.[5]

* Corresponding author. Fax: +351 212948385. Tel: +351 212949658. E-mail: hrg@dq.fct.unl.pt.
† Present address: CQM-Centro de Química da Madeira, Departamento de Química da Universidade da Madeira, Campus da Penteada, 9000-390 Funchal, Portugal.

The speed of sound (u) is a thermodynamic property that can be experimentally determined with great accuracy over a large range of temperature and pressure conditions, both in the liquid and in the gas phases. Since u can be related to the first pressure partial derivative of the density, high accuracy speed of sound data can be used to enhance the development of equations of state (EOS). Also, it is very useful as a source of information to compute the values of other thermodynamic properties difficult to obtain at extreme experimental conditions, such as calorimetric data at high pressures. In the present work, the ultrasonic speed of propagation in liquid R410A has been measured with an apparatus designed to operate at high pressures. This apparatus has been tested and the results reported for other alternative refrigerants.[7–11] The experimental data were fitted and used together with density and isobaric heat capacity data from REFPROP[12] to calculate, through an integration method,[7,13–15] several thermodynamic properties such as the isentropic and isothermal compressibilities (κ_S and κ_T), the isobaric thermal expansion coefficient (α_p), the thermal pressure coefficient (γ_V), the isenthalpic Joule–Thomson coefficient (μ_{JT}), the isobaric and isochoric heat capacities (C_p and C_V), and enthalpy and entropy variations relative to a reference state.

Recent works have shown that it seems likely that blends of new refrigerants rather than pure substances will replace the common CFCs. Vapor–liquid equilibrium data are required in order to evaluate the performance of refrigeration cycles. Moreover, apart from other important physicochemical properties, the knowledge of critical parameters is essential to design a simple process. Mixtures of partially fluorinated gases with CO$_2$ can be used as refrigerants or as modifiers to improve solubility in supercritical fluids. Therefore, knowledge of their phase behavior is crucial. In this work, critical properties of the refrigerant R410A and their mixtures with CO$_2$ were investigated. To that end, we have applied an acoustic simple technique that proved to be a reliable method to explore the

Table 1. Experimental Speed of Sound, u/m·s⁻¹, for Alternative Refrigerant Mixture R410A as a Function of Temperature T and Pressure p

T = 253.09 K		T = 258.09 K		T = 265.61 K		T = 273.12 K		T = 280.72 K		T = 288.20 K		T = 298.20 K		T = 308.25 K		T = 318.17 K	
p	u	p	u	p	u	p	u	p	u	p	u	p	u	p	u	p	u
MPa	m·s⁻¹	MPa	m·s⁻¹	MPa	m·s⁻¹	MPa	m·s⁻¹	MPa	m·s⁻¹	MPa	m·s⁻¹	MPa	m·s⁻¹	MPa	m·s⁻¹	MPa	m·s⁻¹
1.18	684.1	1.00	656.5	1.19	618.9	0.83	574.5	1.03	535.2	1.35	496.0	1.68	440.6	2.17	383.3	2.75	323.4
1.26	684.8	1.12	657.6	1.34	620.0	0.83	574.5	1.06	535.5	1.42	497.2	1.68	440.2	2.17	383.4	2.76	323.6
1.38	685.8	1.26	658.8	1.50	621.6	1.22	578.8	1.15	536.9	.148	498.0	1.68	440.3	2.25	384.9	2.88	327.2
1.50	686.8	1.38	659.7	1.75	623.8	1.36	580.1	1.26	538.0	1.55	499.0	1.75	441.7	2.38	387.7	3.01	330.8
1.62	687.7	1.50	660.8	2.01	626.1	1.50	581.6	1.38	539.4	1.65	500.3	1.88	444.0	2.51	390.5	3.25	337.8
1.75	688.8	1.50	661.0	2.25	628.3	1.75	584.2	1.50	540.9	1.75	501.7	2.01	446.0	2.75	395.6	3.50	344.5
2.01	690.6	1.63	662.2	2.51	630.7	2.01	586.8	1.63	542.3	1.88	503.4	2.13	448.2	3.01	400.6	4.00	356.6
2.25	692.6	1.75	663.1	2.75	633.0	2.25	589.4	1.75	543.8	2.01	505.1	2.25	450.0	3.50	409.9	4.50	367.9
2.51	694.3	2.01	665.1	3.01	635.2	2.51	591.9	2.01	546.7	2.25	508.2	2.51	454.0	4.00	418.9	5.00	378.2
2.75	696.4	2.25	667.1	3.50	639.4	2.75	594.1	2.25	549.6	2.51	511.3	2.75	457.8	4.50	427.4	6.01	397.4
3.01	698.4	2.51	669.2	4.00	644.0	3.01	596.9	2.51	552.3	2.75	514.7	3.01	461.7	5.00	435.6	7.01	414.5
3.50	702.3	2.75	671.4	4.50	648.1	3.50	601.6	2.75	555.0	3.01	517.7	3.50	469.1	6.01	450.5	8.00	429.7
4.00	705.0	3.01	673.4	5.00	652.1	4.00	606.4	3.01	557.9	3.50	524.0	4.00	475.9	7.01	464.7	9.00	444.1
4.50	709.5	3.50	677.1	6.01	660.6	4.50	611.0	3.50	563.2	4.00	529.7	4.50	483.0	8.00	477.8	10.00	457.3
5.00	713.3	4.00	681.1	7.01	668.4	5.00	615.4	4.00	568.5	4.50	535.6	5.00	489.9	9.00	490.2	12.00	481.7
6.01	720.6	4.50	685.3	8.00	676.1	6.01	624.4	4.50	573.7	5.00	541.1	6.01	502.6	10.00	501.7	14.00	503.8
7.01	727.4	5.00	689.1	9.00	683.8	7.01	633.3	5.00	579.0	6.01	552.0	7.01	514.4	12.00	523.6	16.01	524.3
8.00	734.2	6.01	696.6	10.00	691.0	8.00	641.5	6.01	588.6	7.01	562.3	8.00	525.7	14.00	543.5	18.00	543.1
9.00	740.8	7.01	703.9	12.00	705.2	9.00	649.3	7.01	598.3	8.00	572.3	9.00	536.4	16.01	562.1	20.00	560.6
10.00	747.5	8.00	711.0	14.00	718.9	10.00	657.6	8.00	607.1	9.00	582.0	10.00	546.7	18.00	579.5	23.00	585.3
12.00	760.2	9.00	718.1	16.01	732.1	12.00	672.7	9.00	615.9	10.00	591.2	12.00	566.4	20.00	596.0	26.00	607.9
14.00	772.5	10.00	724.8	18.00	744.4	14.00	687.3	10.00	624.5	12.00	608.7	14.00	584.5	23.00	619.0	29.01	628.9
16.01	784.5	12.00	738.2	20.00	756.2	16.01	701.1	12.00	640.6	14.00	625.1	16.01	601.6	26.00	640.0	32.00	648.5
18.00	795.3	14.00	751.2	23.00	773.6	18.00	714.5	14.00	656.1	16.01	640.6	18.00	617.3	29.01	660.1	35.00	667.3
20.00	806.9	16.01	763.4	26.00	790.1	20.00	727.0	16.01	670.9	18.00	655.7	20.00	632.4	32.00	678.9	40.00	696.7
23.00	822.9	18.00	775.0	29.01	806.2	23.00	745.4	18.00	684.9	20.00	669.7	23.00	653.8	35.00	697.2	45.00	723.8
26.00	837.9	20.00	786.7	32.00	821.5	26.00	762.7	20.00	698.3	23.00	689.6	26.00	673.7	40.00	725.2	50.00	749.1
29.01	852.8	23.00	803.2	35.00	835.5	29.01	779.0	23.00	717.0	26.00	708.7	29.01	693.0	45.00	751.3	55.00	772.8
32.00	867.2	26.00	818.7	40.00	858.8	32.00	794.8	26.00	735.5	29.01	727.0	32.00	711.1	50.00	775.7	60.00	795.7
35.00	880.5	29.01	833.7	45.00	880.8	35.00	809.6	29.01	752.6	32.00	744.0	35.00	728.5	55.00	798.8	65.00	817.3
40.00	902.6	32.00	848.7	50.00	902.0	40.00	833.5	32.00	769.2	35.00	760.4	40.00	754.9	60.00	821.0		
45.00	923.6	35.00	862.6	55.00	922.4	45.00	856.4	35.00	785.1	40.00	786.1	45.00	780.3	65.00	841.9		
50.00	943.8	40.00	885.0	60.00	941.6	50.00	877.8	40.00	809.7	45.00	810.0	50.00	803.7				
55.00	962.8	45.00	906.3	65.00	959.9	55.00	898.7	45.00	833.1	50.00	833.0	55.00	826.3				
60.00	981.2	50.00	926.7			60.00	919.0	50.00	855.5	55.00	854.6	60.00	847.6				
65.00	999.5	55.00	946.6			65.00	938.0	55.00	876.4	60.00	875.4	65.00	868.2				
		60.00	965.6					60.00	898.9	65.00	895.5						
		65.00	983.3					65.00	916.7								

	T = 328.17 K					T = 338.16 K		
	p	u	p	u		p	u	p	u
	MPa	m·s⁻¹	MPa	m·s⁻¹		MPa	m·s⁻¹	MPa	m·s⁻¹
	3.47	257.9	14.00	464.8		4.34	183.3	18.00	472.9
	3.47	258.1	16.01	487.3		4.41	189.7	20.00	493.2
	3.47	258.0	18.00	507.4		4.50	200.4	23.00	521.1
	3.59	263.4	20.00	526.4		4.75	217.6	26.00	546.3
	3.72	269.8	23.00	552.3		5.00	231.3	29.01	569.7
	3.86	275.4	26.00	576.7		5.50	255.4	32.00	591.3
	4.00	281.3	29.01	598.7		6.01	273.8	35.00	611.3
	4.25	290.2	32.00	619.2		7.01	303.5	40.00	642.8
	4.50	298.5	35.00	638.6		8.00	327.5	45.00	671.7
	5.00	313.4	40.00	669.0		9.00	348.4	50.00	698.8
	6.01	339.3	45.00	697.4		10.00	366.8	55.00	724.1
	7.01	360.6	50.00	723.3		12.00	398.9	60.00	747.7
	8.00	379.4	55.00	747.8		14.00	426.3	65.00	770.1
	9.00	396.7	60.00	770.9		16.01	450.8		
	10.00	412.2	65.00	793.1					
	12.00	440.2							

critical behavior of multicomponent systems as reported in previous works.[11,16−23] Measurements of the critical temperature T_c and pressure p_c of the CO_2 + R410A mixtures were performed over the whole composition range. The Peng−Robinson equation of state (PR EOS), with conventional mixing and combining rules, was used to correlate the experimental data.

Experimental Section

Materials. The R410A used in the experimental work was supplied by Solvay Fluor und Derivate GmbH, with a stated composition of 50 wt % of pentafluoroethane (R125) + 50 wt % of difluoromethane (R32). CO_2 was supplied by Air Liquide and had a stated purity greater than 99.99 %. The mixtures were prepared in small stainless steel cylinders, and the compositions were determined by weighing.

Speed of Sound Measurements. The speed of sound of liquid R410A was measured using an apparatus designed for high pressures, with an acoustic cell placed inside a stainless steel container, using a pulse-echo method at a frequency of 1 MHz as previously described.[7−11] The cell calibration was performed by measuring the speed of sound of pure CCl_4 at 10 MPa and 298.15 K and comparing the obtained value with data reported

in the literature.[24,25] To cover the complete experimental temperature and pressure ranges, the calibration was expanded by the use of the thermal and pressure behavior of the pure copper spacers (purity better than 99.99 %). The steel container and the acoustic cell were thermostated inside a Dewar vessel within the temperature range from (253 to 388) K, with a control system based on two-stage cascaded thermostatic baths. The long-term stability of the complete system was within ± 0.02 K in the whole range, and the temperature measurements were taken with a four-wire platinum resistance thermometer previously calibrated to an uncertainty of ± 0.01 K on ITS 90 scale. Pressure measurements were performed in two separate ranges with Setra Systems Inc. pressure transducers, one from vapor pressure to 35 MPa and the other up to 65 MPa. The pressure sensors were calibrated against a dead weight gauge with an uncertainty of ± 0.025 MPa in the lower range and ± 0.076 MPa in the higher range.

Taken into account all the error sources, the accuracy of the speed of sound measurements is estimated to be better than ± 0.3 m·s^{-1}. Several measurements were repeated at the same pressure and temperature conditions, allowing us to estimate a precision of ± 0.1 m·s^{-1}.

Measurements of Critical Data. The experimental apparatus for the critical data acquisition has already been described in detail[18,19] and was used unmodified in this study.

The acoustic cell is constructed from a stainless steel 3/8 in. cross piece, with its inner diameter bored out to provide an acoustic cavity of about 5 mL volume. Pressure was generated via a hand pump (High-Pressure Equipment Co., model 62-6-10) and monitored with a pressure transducer (Omega, model PX931) with a precision of ± 0.01 MPa. Temperature was measured on the ITS-90 with a precision of ± 0.001 K with a calibrated platinum resistance thermometer (Tinsley) connected to a digital multimeter (Keithley, model 2000). A pulse generator (Wavetek, model 80) provided the acoustic signal, with a frequency of about 300 kHz. The signal was fed into the acoustic cavity via a piezoelectric ceramic transducer disk (Morgan Matroc Ltd., PC4D) with a thickness of 2 mm and a diameter of 6 mm. A second, identical transducer monitored the signal at the other end of the cavity. The transit times of the pulse across the acoustic cavity were displayed in an oscilloscope (Tektronix, model TDS-340). The acoustic cell was immersed in a 40 L water bath, thermostated with a refrigeration unit and a temperature controller from Hart Scientific, with a RTD probe. This unit provides a temperature control within ± 0.004 K.

A mixture with a desired composition was obtained by weighing and was pumped into the acoustic cell. The pressure was increased with the hand pump until only minute changes in the acoustic signal were observed, meaning that a liquid like state with a low compressibility was present in the acoustic cell. The system was allowed to equilibrate for at least 30 min at the desired starting temperature. Experiments were carried out at constant temperature, and pressure was lowered until a maximum in time delay was observed. Temperature was then systematically varied, and the procedure was repeated. The temperature and pressure values corresponding to the absolute maximum of time delay in the ensemble of the isothermal curves (t_{delay}/μs vs p/MPa) were taken as the critical temperature and critical pressure.

Results and Discussion

Speed of Sound of Liquid R410A. The apparatus was used to take a total of 376 experimental speed of sound measurements
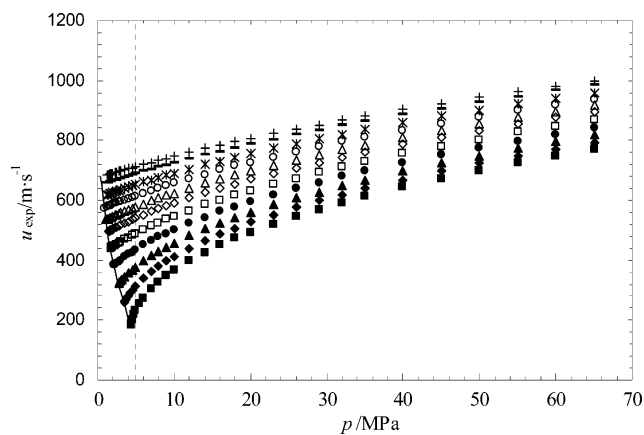

Figure 1. Experimental speed of sound, u, for R410A as a function of pressure at: +, 253.09 K; −, 258.09 K; ∗, 265.61 K; ○, 273.12 K; △, 280.72 K; ◇, 288.20 K; □, 298.20 K; ●, 308.25 K; ▲, 318.17 K; ♦, 328.17 K; ■, 338.16 K; —, saturation line; - - -, critical pressure.

Table 2. Orthobaric Speed of Sound Data for R410A

T	p_σ	u_σ	T	p_σ	u_σ
K	MPa	m·s^{-1}	K	MPa	m·s^{-1}
253.09	0.40	677.8*	298.20	1.65	440.4
258.09	0.48	652.1*	308.25	2.14	383.4
265.61	0.62	613.2*	318.17	2.72	323.4
273.12	0.80	574.5	328.17	3.43	256.3*
280.72	1.01	535.2	338.16	4.28	177.4*
288.20	1.26	494.9*			

a An asterisk (*) indicates an extrapolated value.

of the alternative refrigerant mixture R410A, within the temperature range from (253 to 338) K and pressure range up to 65 MPa. These data are shown in Table 1. The measurements were performed and organized as isotherms, within a total of 11, and are plotted in Figure 1. The consistency of the individual isotherms was tested by fitting each one with

$$u = \sum_{i=0}^{2} A_i[\ln(p - B_i)]^i \qquad (1)$$

The standard deviations of the fits are smaller than 0.18 m·s^{-1} for isotherms in which the reduced temperature is lower than 0.93. For the isotherms at (328 and 338) K, which correspond to reduced temperatures of 0.95 and 0.98, the standard deviations of the fits are 0.32 m·s^{-1} and 0.67 m·s^{-1}, respectively. This increase in the standard deviation of the fits can be explained by the proximity of the critical temperature and consequently abrupt changes in the speed of sound measures when we are close to the critical point, as can be seen in Figure 1.

It was possible to measure the saturated liquid (orthobaric) speed of sound, u_σ, for the isotherms between 273 K and 318 K except for 288 K. In the cases where the direct measurement was not possible, eq 1 was used to extrapolate the speed of sound at this temperature to the vapor pressure (REFPROP).[12] The orthobaric speed of sound data presented in Table 2 were fitted to

$$u_\sigma = \sum_{i=0}^{4} a_i \left[\ln\left(\frac{T}{T_c}\right) \right]^i \qquad (2)$$

(critical data T_c = 344.90 K, measured value in this work) with the coefficients of Table 3. The standard deviation of the fit was 0.70 m·s^{-1}.

Table 3. Coefficients of Equation 2 for the Orthobaric Speed of Sound, u_σ

i	a_i	i	a_i
0	1.182664E+02	3	−2.735656E+04
1	−3.183315E+03	4	−3.057635E+04
2	−9.987818E+03		

Table 4. Coefficients of Equation 3 for the Speed of Sound of R410A, Valid from $T = (253$ to $338)$ K and Pressures from Saturation up to 65 MPa

a_{ij}	j		
i	0	1	2
0	1.7954580E+03	−1.0022012E+01	1.3836079E−02
1	−6.2369087E+01	4.6733643E−01	−8.0659148E−04
2	1.9859669E−01	−3.0301947E−03	8.9030601E−06

b_{kl}	l		
k	0	1	2
0	1	−3.3868948E−03	1.1342597E−06
1	−4.5482056E−02	2.6896918E−04	−2.9582158E−07
2	4.5276779E−04	−4.4360736E−06	1.0375652E−08

Finally, the set of experimental data excluding the isotherm at 338 K, was fitted to

$$u = \frac{\sum_{i=0}^{2}\sum_{j=0}^{2} a_{ij}p^i T^j}{\sum_{k=0}^{2}\sum_{l=0}^{2} b_{kl}p^k T^l} \quad (3)$$

with the coefficients shown in Table 4 and a standard deviation of 0.40 m·s⁻¹. The comparison between our fitted speed of sound data and the results obtained from REFPROP[12] are presented in Figure 2. The deviations are slightly high, but this can be related with the mixing rule used in the commercial package. As far as we are aware of there are no other speed of sound experimental data to which the present work can be compared.

Derived Thermodynamic Properties. The speed of sound, u, is directly related to the pressure derivative of the density, ρ, through eq 4, in which the subscript S denotes the condition of constant entropy:

$$\left(\frac{\partial\rho}{\partial p}\right)_S = \frac{1}{u^2} \quad (4)$$

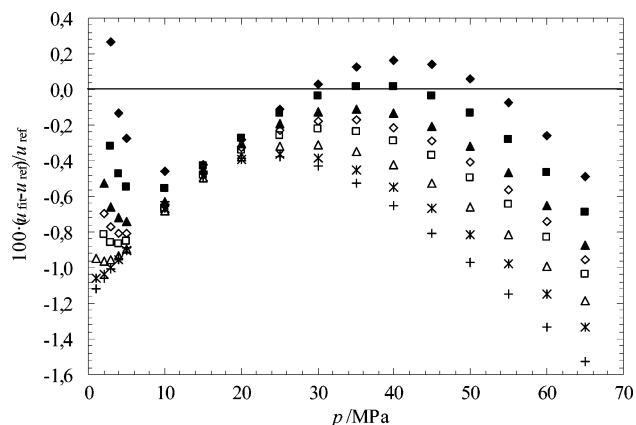This derivative is related to the isothermal pressure derivative

Figure 2. Percentage deviations $\{100\cdot(u_{fit} - u_{ref}/u_{ref}\}$ of the calculated speed of sound, u_{fit}, to REFPROP[12] data, u_{ref}. of R410A: +, 260 K; ∗, 270 K; △, 280 K; □, 290 K; ◇, 295 K; ▲, 300 K; ■, 310 K; ◆, 320 K.

Table 5. Coefficients Used To Fit the Literature Density, ρ_i, and Heat Capacity Data, C_j, with Equationss 14 and 15, Respectively

i	d_i	c_i
0	6.635945E+04	−1.260861E+07
1	−1.191944E+03	3.285457E+05
2	8.778011E+00	−3.662179E+03
3	−3.237582E−02	2.263942E+01
4	5.969828E−05	−8.383379E−02
5	−4.408465E−08	1.859637E−04
6		−2.288239E−07
7		1.204971E−10

and the isobaric temperature derivative of the density through eq 5, where C_p is the specific heat capacity at constant pressure:

$$\left(\frac{\partial\rho}{\partial p}\right)_S = \left(\frac{\partial\rho}{\partial p}\right)_T - \frac{T}{\rho^2\cdot C_p}\left(\frac{\partial\rho}{\partial T}\right)_p^2 \quad (5)$$

Rearranging the last equation and combining it with eq 4, follows eq 6, which also incorporates the definition of the thermal expansion coefficient, α_p:

$$\left(\frac{\partial\rho}{\partial p}\right)_T = \frac{1}{u^2} + \frac{T}{C_p}\cdot\alpha_p^2 \quad (6)$$

$$\alpha_p = -\frac{1}{\rho}\left(\frac{\partial\rho}{\partial T}\right)_p \quad (7)$$

It can also be shown that the pressure partial derivative of the isobaric heat capacity can calculated with eq 8:

$$\left(\frac{\partial C_p}{\partial p}\right)_T = -\frac{T}{\rho}\left[\alpha_p^2 + \left(\frac{\partial\alpha_p}{\partial T}\right)_p\right] \quad (8)$$

This way, given an isobar of the density and of C_p, it is possible to integrate eqs 6 and 8 over the pressure thus obtaining the (p, ρ, T) and (p, C_p, T) surfaces within the range of pressure and temperature of the experimental speed of sound data. The numerical integration procedure also allows, through the use of eqs 9 to 13, the calculation of other properties, such as the isentropic compressibility κ_S; the isothermal compressibility κ_T; the isochoric heat capacity C_v; the thermal pressure coefficient γ_v; and the isenthalpic Joule−Thomson coefficient μ_{JT}:

$$\kappa_S = \frac{1}{\rho\cdot u^2} \quad (9)$$

$$\kappa_T = \frac{1}{\rho}\left(\frac{\partial\rho}{\partial p}\right)_T \quad (10)$$

$$C_v = \frac{C_p}{\gamma} \quad (11)$$

$$\gamma_v = \frac{\alpha_p}{\kappa_T} \quad (12)$$

$$\mu_{JT} = \frac{T\cdot\alpha_p - 1}{\rho\cdot C_p} \quad (13)$$

In the present work, because the available experimental density is scarce and no isobaric heat capacity data exist, the authors used data from the commercial available program REFPROP[12] at a pressure of 5 MPa and temperatures from (240

Table 6. Calculated Densities ρ for R410A as a Function of Temperature T and Pressure p

	$\rho/(\text{kg} \cdot \text{m}^{-3})$							
p/MPa	$T = 260$ K	$T = 270$ K	$T = 280$ K	$T = 290$ K	$T = 295$ K	$T = 300$ K	$T = 310$ K	$T = 320$ K
1.0	1223.1	1184.6	1142.8					
3.0	1231.0	1194.1	1154.4	1111.5	1088.4	1063.8	1008.2	937.6
5.0	1238.4	1202.8	1165.0	1124.5	1103.1	1080.5	1031.2	973.2
10.0	1255.1	1222.5	1188.1	1152.1	1133.3	1114.1	1073.6	1029.7
15.0	1270.1	1239.6	1207.8	1174.8	1157.9	1140.6	1105.0	1067.8
20.0	1283.5	1254.9	1225.2	1194.4	1178.7	1162.9	1130.5	1097.3
25.0	1295.9	1268.7	1240.7	1211.8	1197.1	1182.2	1152.2	1121.7
30.0	1307.3	1281.4	1254.8	1227.4	1213.5	1199.4	1171.1	1142.7
35.0	1317.9	1293.1	1267.7	1241.6	1228.3	1215.0	1188.1	1161.2
40.0	1327.9	1304.1	1279.7	1254.7	1242.0	1229.2	1203.5	1177.9
45.0	1337.3	1314.3	1290.8	1266.8	1254.6	1242.4	1217.7	1193.1
50.0	1346.2	1323.9	1301.3	1278.2	1266.4	1254.6	1230.8	1207.1
55.0	1354.7	1333.0	1311.1	1288.8	1277.5	1266.1	1243.0	1220.1
60.0	1362.8	1341.7	1320.5	1298.9	1287.9	1276.8	1254.5	1232.3
65.0	1370.6	1349.9	1329.3	1308.4	1297.8	1287.0	1265.4	1243.7

Table 7. Calculated Isobaric Heat Capacity C_p for R410A as a Function of Temperature T and Pressure p

	$C_p/(\text{J} \cdot \text{kg}^{-1} \cdot \text{K}^{-1})$							
p/MPa	$T = 260$ K	$T = 270$ K	$T = 280$ K	$T = 290$ K	$T = 295$ K	$T = 300$ K	$T = 310$ K	$T = 320$ K
1.0	1447	1490	1543					
3.0	1432	1469	1514	1575	1615	1664	1805	2057
5.0	1418	1451	1490	1541	1572	1608	1701	1848
10.0	1388	1414	1446	1482	1502	1523	1566	1621
15.0	1363	1386	1413	1443	1459	1473	1499	1522
20.0	1343	1363	1387	1415	1428	1440	1457	1468
25.0	1326	1343	1366	1392	1404	1416	1430	1434
30.0	1312	1327	1348	1373	1385	1397	1410	1411
35.0	1301	1312	1332	1357	1369	1381	1395	1396
40.0	1292	1300	1317	1342	1355	1367	1382	1384
45.0	1286	1289	1305	1329	1342	1355	1372	1375
50.0	1281	1280	1293	1317	1331	1344	1363	1368
55.0	1279	1272	1282	1305	1320	1333	1355	1362
60.0	1278	1266	1273	1295	1309	1324	1347	1357
65.0	1280	1262	1265	1285	1299	1314	1339	1352

to 330) K. These isobars were fitted to eqs 14 and 15 with the coefficients of Table 5:

$$\rho(T, 5 \text{ MPa}) = \sum_{i=0}^{5} d_i \cdot T^i \qquad (14)$$

$$C_p(T, 5 \text{ MPa}) = \sum_{j=0}^{7} c_j \cdot T^j \qquad (15)$$

The integration procedure was implemented both on increasing pressure, up to 65 MPa, and on decreasing pressure down to the saturation line.
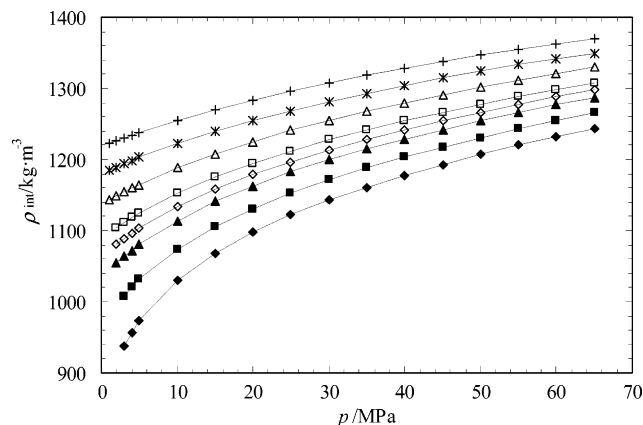
The whole (p, ρ, T) surface obtained from the integration procedure previously described is shown in Figure 3 and Table 6. To test the results, the whole set of calculated density data were fitted with an equation similar to eq 3, with a standard deviation of 0.008 %. Figure 4 shows the percentage deviations between experimental density data[26] and the density data obtained by integration. From this figure, it is possible to see that all the deviations are roughly within ± 0.2 % with the exception of the isotherm at 263.15 K where the deviations are higher. Not shown in Figure 4 there are also density data[27] that are within −0.1 % and +0.3 % from our integration procedure. The complete (p, C_p, T) surface is plotted in Figure 5 and Table 7. The other calculated thermodynamic
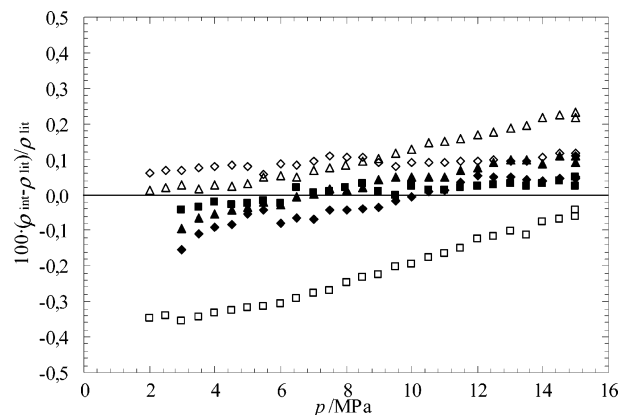

Figure 3. Density data of R410A calculated through the integration procedure as a function of pressure: +, 260 K; *, 270 K; △, 280 K; □, 290 K; ◇, 295 K; ▲, 300 K; ■, 310 K; ◆, 320 K.

Figure 4. Plot of deviations between our results and the literature experimental densities. Piao et al.:[26] □, 263.15 K; △, 273.15 K; ◇, 283.15 K; ■, 293.15 K; ▲, 303.15 K; ◆, 313.15 K.
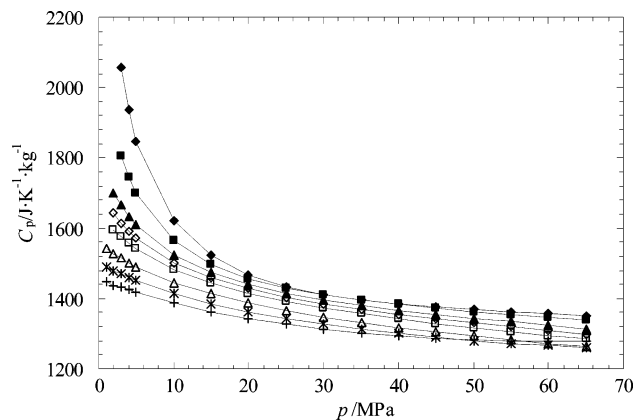
Figure 5. Isobaric heat capacity, C_p, of R410A calculated through the integration procedure: $+$, 260 K; $*$, 270 K; $\triangle$, 280 K; $\square$, 290 K; $\diamond$, 295 K; $\blacktriangle$, 300 K; $\blacksquare$, 310 K; $\blacklozenge$, 320 K.

Figure 7. Isentropic compressibility, κ_S, of R410A calculated through the integration procedure: $+$, 260 K; $*$, 270 K; $\triangle$, 280 K; $\square$, 290 K; $\diamond$, 295 K; $\blacktriangle$, 300 K; $\blacksquare$ 310 K; $\blacklozenge$, 320 K.

Figure 6. Thermal expansion coefficient, α_p, of R410A calculated through the integration procedure: $+$, 260 K; $*$, 270 K; $\triangle$, 280 K; $\square$, 290 K; $\diamond$, 295 K; $\blacktriangle$, 300 K; $\blacksquare$ 310 K; $\blacklozenge$, 320 K.
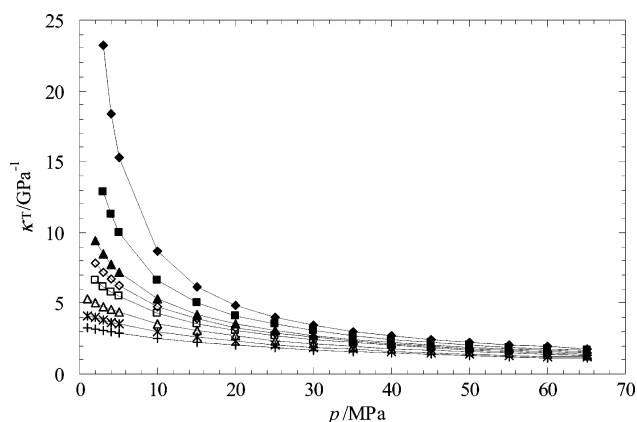
Figure 8. Isothermal compressibility, κ_T, of R410A calculated through the integration procedure: $+$, 260 K; $*$, 270 K; $\triangle$, 280 K; $\square$, 290 K; $\diamond$, 295 K; $\blacktriangle$, 300 K; $\blacksquare$, 310 K; $\blacklozenge$, 320 K.

properties are represented in Figures 6 through 8 and Tables 8 to 10.

Critical Behavior. Our acoustic method was applied to investigate the critical properties of R410A and CO_2 + R410A system. The refrigerant used in this study is a binary azeotropic mixture, which means that its behavior is similar to that one of a pure component. We have considered R410A as a pure component and treated the mixture with CO_2 as a binary mixture and not a ternary one. The estimated errors of the critical parameters reported are $\pm$ 0.1 K for the critical temperature and 0.05 MPa for the critical pressure. The estimate was based on a comparison of the results of different experiments
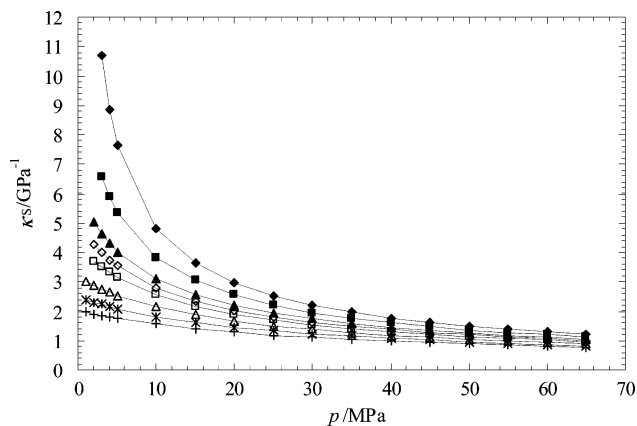
performed with the same mixture and is mainly determined by the narrowness of the isotherms studied as during an experiment the pressure decreases in a continuous way.

R410A. The acoustic experiments are carried out at constant temperature, and the pressure is lowered until a maximum in time delay is observed, meaning that it has reached a local maximum in the compressibility, corresponding to a phase transition. The temperature is then systematically varied and the procedure repeated. Several isotherms were measured in the vicinity of the critical temperature. The temperature and pressure values corresponding to the absolute maximum of time delay

Table 8. Calculated Isobaric Thermal Expansion Coefficient α_p for R410A as a Function of Temperature T and Pressure p

	$\alpha_p \cdot 10^3 / K^{-1}$							
p/MPa	$T = 260$ K	$T = 270$ K	$T = 280$ K	$T = 290$ K	$T = 295$ K	$T = 300$ K	$T = 310$ K	$T = 320$ K
1.0	3.025	3.383	3.822					
3.0	2.918	3.196	3.567	4.044	4.364	4.780	6.112	8.682
5.0	2.784	3.046	3.355	3.737	3.980	4.278	5.134	6.576
10.0	2.534	2.741	2.962	3.209	3.350	3.509	3.908	4.476
15.0	2.342	2.510	2.683	2.862	2.956	3.057	3.287	3.583
20.0	2.187	2.327	2.469	2.610	2.680	2.750	2.898	3.071
25.0	2.059	2.176	2.298	2.415	2.470	2.524	2.626	2.734
30.0	1.952	2.049	2.155	2.258	2.304	2.347	2.424	2.493
35.0	1.861	1.941	2.035	2.126	2.167	2.204	2.265	2.312
40.0	1.783	1.847	1.930	2.014	2.051	2.084	2.136	2.169
45.0	1.717	1.765	1.838	1.916	1.951	1.982	2.027	2.052
50.0	1.660	1.693	1.757	1.829	1.862	1.892	1.934	1.955
55.0	1.611	1.629	1.684	1.751	1.783	1.811	1.853	1.871
60.0	1.570	1.573	1.618	1.681	1.711	1.739	1.780	1.798
65.0	1.535	1.522	1.559	1.616	1.646	1.673	1.715	1.732

Table 9. Calculated Isentropic Compressibility κ_S for R410A as a Function of Temperature T and Pressure p

	κ_S/GPa^{-1}							
p/MPa	T = 260 K	T = 270 K	T = 280 K	T = 290 K	T = 295 K	T = 300 K	T = 310 K	T = 320 K
1.0	1.955	2.394	3.014					
3.0	1.844	2.228	2.749	3.491	3.991	4.621	6.555	10.690
5.0	1.748	2.087	2.534	3.145	3.539	4.016	5.347	7.619
10.0	1.552	1.813	2.139	2.554	2.806	3.094	3.814	4.805
15.0	1.403	1.612	1.865	2.175	2.356	2.557	3.035	3.643
20.0	1.284	1.458	1.663	1.906	2.045	2.197	2.547	2.972
25.0	1.187	1.334	1.505	1.703	1.815	1.935	2.206	2.525
30.0	1.106	1.233	1.378	1.544	1.636	1.734	1.953	2.204
35.0	1.036	1.148	1.274	1.415	1.493	1.576	1.757	1.961
40.0	0.976	1.075	1.186	1.309	1.376	1.446	1.600	1.771
45.0	0.924	1.012	1.110	1.219	1.277	1.339	1.472	1.618
50.0	0.877	0.957	1.045	1.142	1.194	1.248	1.365	1.492
55.0	0.835	0.908	0.988	1.076	1.122	1.171	1.275	1.387
60.0	0.797	0.864	0.938	1.017	1.060	1.104	1.197	1.298
65.0	0.763	0.825	0.893	0.966	1.005	1.045	1.130	1.221

Table 10. Calculated Isothermal Compressibility κ_T for R410A as a Function of Temperature T and Pressure p

	κ_T/GPa^{-1}							
p/MPa	T = 260 K	T = 270 K	T = 280 K	T = 290 K	T = 295 K	T = 300 K	T = 310 K	T = 320 K
1.0	3.299	4.144	5.334					
3.0	3.101	3.800	4.787	6.200	7.187	8.493	12.918	23.195
5.0	2.895	3.522	4.349	5.482	6.233	7.175	10.006	15.314
10.0	2.511	2.986	3.569	4.303	4.750	5.271	6.629	8.647
15.0	2.227	2.602	3.046	3.576	3.882	4.225	5.058	6.170
20.0	2.006	2.312	2.667	3.075	3.303	3.551	4.126	4.845
25.0	1.829	2.084	2.377	2.706	2.885	3.076	3.504	4.012
30.0	1.683	1.900	2.148	2.421	2.568	2.721	3.055	3.438
35.0	1.561	1.747	1.960	2.194	2.317	2.444	2.716	3.017
40.0	1.458	1.619	1.804	2.007	2.113	2.222	2.450	2.694
45.0	1.369	1.509	1.672	1.851	1.944	2.039	2.234	2.439
50.0	1.292	1.414	1.559	1.718	1.801	1.885	2.056	2.233
55.0	1.225	1.330	1.460	1.604	1.679	1.754	1.907	2.061
60.0	1.165	1.257	1.374	1.504	1.572	1.641	1.779	1.916
65.0	1.112	1.192	1.297	1.417	1.479	1.542	1.668	1.792

Table 11. Experimental Critical Data, p_c and T_c, of the System CO_2 + R410A

x_{CO_2}	p_c/MPa	T_c/K	x_{CO_2}	p_c/MPa	T_c/K
0.979	7.39	306.45	0.501	6.35	328.95
0.951	7.35	307.75	0.254	5.84	336.10
0.919	7.32	309.03	0.100	5.30	341.05
0.902	7.27	311.32	0.053	5.01	343.45
0.855	7.16	314.50	0.000	4.90	344.90
0.746	6.97	319.86			

in the ensemble of the isothermal curves is taken as the critical temperature and pressure.

The experimental critical point of the azeotropic mixture R410A was determined by different authors.[28,29] Nagel and Bier reported the values T_c = 344.75 K and p_c = 4.93 MPa. Kishizawa et al.[6] determined a slightly lower critical temperature (344.48 K) for R410A by observation of the critical opalescence. Kato et al.[29] reported the following critical parameters: T_c = 344.63 K and p_c = 4.90 MPa. These data deviate less than 0.1 % in temperature and 0.2 % in pressure from the gas−liquid critical values obtained by our acoustic method: 344.90 K for critical temperature and 4.90 MPa for critical pressure. It can be concluded that the acoustic results measured in our apparatus are in good agreement with the literature values within the combined experimental errors.

CO_2 + R410A. The critical line of CO_2 + R410A mixture was determined over the whole composition range. Acoustic measurements were performed on seven mixtures. The experimental critical parameters, T_c and p_c, are shown in Table 11 for each mixture and are plotted in Figure 9. The system exhibits type I fluid phase behavior, according to the classification of van Konynenburg and Scott,[30] which means that a continuous critical line connects the critical points of R410A and CO_2. This system behaves almost ideally. The projections of critical line are continuous lines connecting the critical points. No maxima or minima in the projections of the critical line are visible. This suggests that R410A should be a useful modifier for CO_2. Its relatively low critical temperature (344.90 K) and its miscibility with CO_2 make it potentially attractive as modifier for improving solubility in supercritical CO_2. As can be seen from Figure 9, the critical pressure of the system goes from p_c of pure CO_2, down to 4.90 MPa, the critical pressure of R410A. This means that as R410A is added to CO_2 the solvation properties of the mixture will have substantially changed, but the critical temperature and critical pressure remain reasonably low. Similar critical behavior was observed in our former study on the CO_2 + R404A system.[11] As it was concluded for R404A, R410A could also conveniently be used to modify CO_2.

Correlation of Data

Experimental critical data were correlated with the PR EOS[31] that is a cubic EOS based on a one-fluid model:

$$p = \frac{RT}{(V_m - b)} - \frac{a(T)}{V_m(V_m + b) + b(V_m - b)} \qquad (16)$$

In its extension to binary mixtures, the characteristic parameters a and b are calculated using the following van der Waals one-fluid mixing rules, which assume random distribution of molecules:

$$a = x_1^2 a_1 + 2x_1 x_2 a_{12} + x_2^2 a_2 \qquad (17)$$

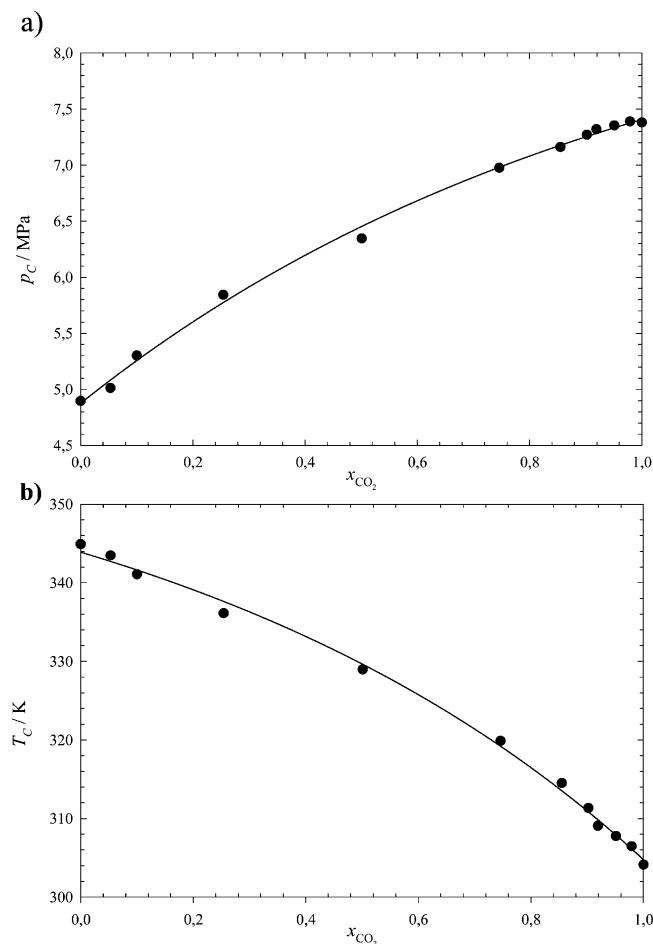$$b = x_1^2 b_1 + 2x_1 x_2 b_{12} + x_2^2 b_2 \qquad (18)$$

a)

b)

Figure 9. Projections of the critical curve for the xCO$_2$ + $(1 - x)$R410A system: (a) $p-x$ projection. (b) $T-x$ projection.

In these equations x_i is the mole fraction of component i ($i = 1, 2$), and a_i and b_i are pure component parameters defined by Peng and Robinson.[31] In particular, $a_i(T) = a_{c,i}(T_{c,i})$ $\alpha_i(T, \beta_i(\omega_i))$, where ω_i is Pitzer's acentric factor of molecule i. The combining rules for the binary cross-interaction parameters a_{12} and b_{12} are given by

$$a_{12} = (a_1 a_2)^{1/2}(1 - k_{12}) \tag{19}$$

$$b_{12} = \frac{1}{2}(b_1 + b_2)(1 - l_{12}) \tag{20}$$

Here k_{12} and l_{12} and parameters describing deviations from, respectively, the geometric and arithmetic mean combining rules. Values of critical temperature, critical pressure and acentric factor[32,33] for each pure fluid, which are presented in Table 12, constitute, along with the deviation parameters, the model input variables for PR EOS. R410A acentric factor was calculated using the definition of Pitzer[34-37] and the experimental data T_c, p_c, and vapor pressures reported by Solvay Technical Data Sheets.[38] The deviation parameters k_{12} and l_{12} were varied so that the theoretical critical line would give the best fit of the experimental data for each binary system. Although the deviation parameters are often fitted to the experimental critical data using only the equimolar mixture,[20] we used all the experimental data available for evaluating these parameters. The deviation parameters of CO$_2$ + R410A that gave the best fit were $k_{12} = 0.0002$ and $l_{12} = 0.015$. Figure 10 shows the (p, T) projection of the critical line for this system using the optimized interaction parameters and the pure component vapor pressures for the
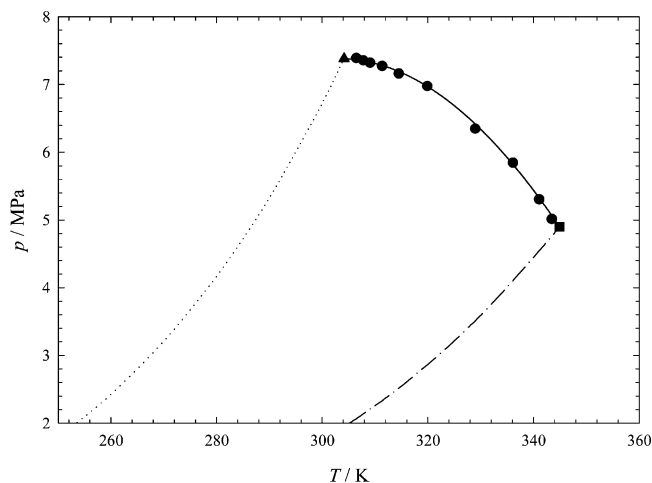

Figure 10. $p-T$ projection of the critical curve for the xCO$_2$ + $(1 - x)$-R410A system: ●, acoustic data; —, predicted critical curve with PR-EOS; - - -, vapor pressure curves for CO$_2$;[33] — · —, vapor pressure curve for R410A.[34]

Table 12. Parameters of CO$_2$ and R410A Used in the Peng−Robinson Equation of State

component	p_C/MPa	T_C/K	ω_i
CO$_2$	7.38[35,36]	304.13[36]	0.239[37]
R410A	4.89[38]	344.95[38]	0.287

binary system. It can be seen from this figure that the PR EOS gives a reasonable agreement with the experimental data for this binary system.

Conclusions

The thermophysical properties and critical parameters for the alternative refrigerant R410A (50 wt % of pentafluoroethane (R125) + 50 wt % of difluoromethane (R32)) were investigated using two different acoustic techniques. The critical behavior of the system xCO$_2$ + $(1 - x)$R410A was also investigated over the whole composition range. With mole fractions of up to 10 % of R410A, critical temperature only increases 7 K, and the critical pressure decreases only 0.1 MPa. The critical line shows type I fluid phase behavior. The results were well-correlated with the PR EOS using conventional mixing and combining rules.

Literature Cited

(1) (a) Koenig, H. *Comparison of R-410A, R-407 and propane in heat pump applications*. IIR Conference, Linz, Austria, 1997. (b) Solvay Fluor und Derivate GmbH, Prod. Bull. C/09.97/04/E.

(2) Dossat, R. J. *Principles of Refrigeration*: Prentice Hall: Upper Saddle River, NJ, 1997.

(3) (a) Hellmann, J.; Doering, R. *Comparison of R22, R410A and R407 in a refrigeration plant*. DKV Conference, Leipzig, Germany, 1996. (b) Solvay Fluor und Derivate GmbH, Prod. Bull. C/11.96/02/E.

(4) Calm, J. M.; Domanski, P. A. R22 replacement status. *ASHRAE J.* **2004**, *46*, 29−39.

(5) Lemmon, E. W.; Jacobsen, R. T. Equations of state for mixtures of R-32, R-125, R-134a, R-143a, and R-152a. *J. Phys. Chem. Ref. Data* **2004**, *33*, 593−620.

(6) Kishizawa, G.; Sato, H.; Watanabe, K. Measurements of saturation densities in critical region and critical loci for binary R-32/125 and R-125/143a systems. *Int. J. Thermophys.* **1999**, *211*, 923−932.

(7) Pires, P. F.; Guedes, H. J. R. The speed of sound and isentropic compressibility of liquid difluoromethane (HFC32) from $T = (248$ to $343)$ K and pressures up to 65 MPa. *J. Chem. Thermodyn.* **1999**, *31*, 55−69.

(8) Pires, P. F.; Guedes, H. J. R. The speed of sound and derived thermodynamic properties of liquid trifluoromethane (HFC23) from $T = (258$ to $303)$ K and pressures up to 65 MPa. *J. Chem. Thermodyn.* **1999**, *31*, 479−490.

(9) Pires, P. F.; Esperança, J. M. S. S.; Guedes H. J. R. Ultrasonic speed of sound and derived thermodynamic properties of liquid 1,1,1,2,3,3,3-heptafluoropropane (HFC227ea) from 248 K to 333 K and pressures up to 65 MPa. *J. Chem. Eng. Data* **2000**, *45*, 496−501.

(10) Gomes de Azevedo, R.; Szydlowski, J.; Pires, P. F.; Esperança, J. M. S. S.; Guedes, H. J. R.; Rebelo, L. P. N. A novel non-intrusive microcell for sound-speed measurements in liquids. Speed of sound and thermodynamic properties of 2-propanone at pressures up to 160 MPa. *J. Chem. Thermodyn.* **2004**, *36*, 211−222.

(11) Esperança, J. M. S. S.; Pires, P. F.; Guedes, H. J. R.; Ribeiro, N.; Costa, T.; Aguiar-Ricardo, A. Acoustic determination of thermophysical properties and critical parameters of R404A and critical line of xCO$_2$ + (1 − x)R404A. *J. Chem. Eng. Data* **2006**, *51*, 1148−1155.

(12) McLinden, M. O.; Klein, S. A.; Lemmon, E. W.; Peskin, A. P. *REFPROP*; NIST Standard Reference Database 23. Version 6.01; Standard Reference Data Program: Gaithersbur, MD, 1998.

(13) Muringer, M. J. P.; Trappeniers, N. J.; Biswas, S. N. The effect of pressure on the sound-velocity and density of toluene and *n*-heptane up to 2600 bar. *Phys. Chem. Liq.* **1985**, *14*, 273−296.

(14) Sun, T.; Biswas, S. N.; Trappeniers, N. J. Seldam; C. A. T. Acoustic and thermodynamic properties of methanol from 273 to 333 K and at pressures up to 280 MPa. *J. Chem. Eng. Data* **1988**, *33*, 395−398.

(15) Daridon, J. L.; Lagrabette, A.; Lagourette, B. Speed of sound, density, and compressibilities of heavy synthetic cuts from ultrasonic measurements under pressure. *J. Chem. Thermodyn.* **1998**, *30*, 607−623.

(16) Kordikowski, A.; Robertson, D. G.; Aguiar-Ricardo, A.; Popov, V. K.; Howdle, S. M.; Poliakoff, M. Probing vapor/liquid equilibria of near-critical binary gas mixtures by acoustic measurements. *J. Phys. Chem.* **1996**, *100*, 9522−9526.

(17) Kordikowski, A.; Robertson, D. G.; Poliakoff, M.; DiNoia, T. D.; McHugh, M.; Aguiar-Ricardo, A. Acoustic determination of the critical surfaces in the ternary systems CO$_2$ + CH$_2$F$_2$ + CF$_3$CH$_2$F and CO$_2$ + C$_2$H$_4$ + CH$_3$CHCH$_2$ and in their binary subsystems. *J. Phys. Chem. B* **1997**, *101*, 5853−5862.

(18) Ribeiro, N.; Casimiro, T.; Duarte, C.; Poliakoff, M.; Nunes da Ponte, M.; Aguiar-Ricardo, A. Vapor−liquid equilibrium and critical line of the CO$_2$ + Xe system. Critical behavior of the CO$_2$ + Xe versus CO$_2$ + *n*-alkanes. *J. Phys. Chem. B* **2000**, *104*, 791−795.

(19) Ribeiro, N.; Aguiar-Ricardo, A. A simple acoustic probe for fluid phase equilibria: application to the CO$_2$ + N(C$_2$H$_5$)$_3$ system. *Fluid Phase Equilib.* **2001**, *185*, 295−303.

(20) Ribeiro, N.; Aguiar-Ricardo, A.; Kordikowski, A.; Poliakoff, M. Acoustic determination of the critical surface of {x_1CO$_2$+ x_2C$_2$H$_6$ + (1 − x_1 − x_2) CHF$_3$}. *Phys. Chem. Chem. Phys.* **2001**, *3*, 1027−1033.

(21) Aguiar-Ricardo, A.; Temtem, M.; Casimiro, T.; Ribeiro, N. A visual acoustic high-pressure cell for the study of critical behavior of non-simple mixtures *Rev. Sci. Instrum.* **2004**, *75*, 3200−3202.

(22) Aguiar-Ricardo, A.; Casimiro, T.; Costa, T.; Leandro, J.; Ribeiro, N. Visual and acoustic investigation of the critical behavior of mixtures of CO$_2$ with a perfluorinated polyether. *Fluid Phase Equilib.* **2006**, *239*, 26−29.

(23) Reis, J. C. R.; Ribeiro, N.; Aguiar-Ricardo, A. Can the speed of sound be used for detecting critical states of fluid mixtures? *J. Phys. Chem. B* **2006**, *110*, 478−484.

(24) Kyohara, O.; Alpin, C. J.; Benson, G. C. Ultrasonic velocities, compressibilities, and heat capacities for binary mixtures of benzene, cyclohexane, and tetrachloromethane at 298.15 K. *J. Chem. Thermodyn.* **1978**, *10*, 721−730.

(25) Lainez, A.; Miller, J. F.; Zollweg, J. A.; Streett, W. B. Volumetric and speed-of-sound measurements for liquid tetrachloromethane under pressure. *J. Chem. Thermodyn.* **1987**, *19*, 1251−1260.

(26) Piao, C.-C.; Iwata, I.; Noguchi, M. Thermodynamic properties of HFC32, HFC125, and HFC134a mixtures. *Fluid Phase Equilib.* **1988**, *150/151*, 313−322.

(27) Benmansour, S.; Richon, D. Vapor-liquid equilibria and densities of a difluoromethane (R-32, 49.8 wt %) + pentafluoroethane (R-125, 50.2 wt %) mixture (R-410A) at temperatures between 253 and 333 K and pressures up to 20 MPa. *ELDATA*: *Int. Electron. J. Phys.-Chem. Data* **1997**, *3*, 149−158,

(28) Nagel, M.; Bier, K. Vapour−liquid equilibrium of ternary mixtures of the refrigerants R32, R125 and R134a. *Int. J. Refrig.* **1995**, *18*, 534−543.

(29) Kato, R.; Shirakawa, K.; Nishiumi, H. Critical locus and Vapor−liquid equilibria of HFC32−HFC125 system. *Fluid Phase Equilib.* **2002**, *194/197*, 995−1008.

(30) van Konynenburg, P. H.; Scott, R. L. Critical lines and phase equilibria in binary van der Waals mixtures. *Philos. Trans. R. Soc. London*, *A* **1980**, *298*, 495−540.

(31) Peng, D.; Robinson, D. A new two-constant equation of state *Ind. Eng. Chem. Fundam.* **1976**, *15*, 59−64.

(32) Sandler, S. I.; Orbey, H.; Lee, B.-I. *Models for Thermodynamic and Phase Equilibria Calculations*; Sandler, S. I., Ed.; Marcel Dekker: New York, 1994; p 87.

(33) Prausnitz, J. M.; Lichtenthaler, R. N.; De Azevedo, E. G. *Molecular Theory of Fluid-Phase Equilibria*, 3rd ed.; Prentice Hall: Upper Saddle River, NJ, 1999; p 718.

(34) Pitzer, K. S. The volumetric and thermodynamic properties of fluids. I. Theoretical basis and virial coefficients *J. Am. Chem. Soc.* **1955**, *77*, 3427−3433.

(35) Angus, S.; Armstrong, B. B.; de Reuck, K. M. *Carbon Dioxide− International Thermodynamic Tables of the Fluid State-3*; IUPAC, Pergamon Press: Oxford, UK, 1976.

(36) Span, R.; Wagner, W. A new equation of state for carbon dioxide covering the fluid region from the triple-point temperature to 1100 K at pressures up to 800 MPa. *J. Phys. Chem. Ref. Data* **1996**, *25*, 1509−1596.

(37) Reid, R. C.; Prausnitz, J. M.; Pauling, B. E. *The Properties of Gases and Liquids*, 4th ed.; McGraw-Hill: New York, 1987.

(38) Technical Data Sheets. http://www.solvay.com.